Quantitative analysis of *TGFBR2* mutations in Marfan-syndrome-related disorders suggests a correlation between phenotypic severity and Smad signaling activity

Daniel Horbelt[1], Gao Guo[2,3], Peter N. Robinson[2,3,4] and Petra Knaus[1,5,*]

[1]Institute for Chemistry-Biochemistry, Freie Universität Berlin, Berlin, 14195, Germany
[2]Institute for Medical Genetics, Charité-Universitätsmedizin Berlin, Berlin, 13353, Germany
[3]Max Planck Institute for Molecular Genetics, Berlin, 14195, Germany
[4]Berlin-Brandenburg Center for Regenerative Therapies (BCRT), Berlin, 13353, Germany
[5]Berlin-Brandenburg School for Regenerative Therapies (BSRT), Berlin, 13353, Germany
*Author for correspondence (knaus@chemie.fu-berlin.de)

Accepted 25 August 2010
Journal of Cell Science 123, 4340-4350

doi:10.1242/jcs.074773

Summary

Mutations in the gene encoding transforming growth factor-beta receptor type II (*TGFBR2*) have been described in patients with Loeys–Dietz syndrome (LDS), Marfan syndrome type 2 (MFS2) and familial thoracic aortic aneurysms and dissections (TAAD). Here, we present a comprehensive and quantitative analysis of *TGFBR2* expression, turnover and TGF-β-induced Smad and ERK signaling activity for nine mutations identified in patients with LDS, MFS2 and TAAD. The mutations had different effects on protein stability, internalization and signaling. A dominant-negative effect was demonstrated for mutations associated with LDS and MFS2. No mutation showed evidence of an immediate cell-autonomous paradoxical activation of TGF-β signaling. There were no cell biological differences between mutations described in patients with LDS and MFS2. By contrast, R460C, which has been found in familial TAAD but not in MFS2 or LDS, showed a less-severe dominant-negative effect and retained residual Smad phosphorylation and transcriptional activity. TAAD is characterized primarily by thoracic aortic aneurysms or dissections. By contrast, MFS2 is characterized by numerous skeletal abnormalities, and patients with LDS additionally can display craniofacial and other abnormalities. Therefore, our findings suggest that the balance between defects in Smad and ERK signaling might be an important determinant of phenotypic severity in disorders related to mutations in *TGFBR2*.

Key words: TGF-beta receptor, Loeys–Dietz syndrome, Marfan syndrome type II, Thoracic aortic aneurysms and dissections, Kinase, Smad

Introduction

Transforming growth factor beta (TGF-β) superfamily signaling plays roles in the morphogenesis of most organs and continues to function in fully developed organisms, where it is required for tissue homeostasis. Among the many cellular processes regulated by TGF-β superfamily signaling are proliferation, differentiation, migration and survival, in various cellular contexts, including embryonic development, angiogenesis and wound healing. TGF-β is also involved in the maintenance of the extracellular matrix (ECM) (Gordon and Blobe, 2008; Wu and Hill, 2009). Excessive TGF-β signaling can promote the production of ECM components and might be associated with fibrotic disorders (Verrecchia and Mauviel, 2002). Marfan syndrome (MFS) is a hereditary disease caused by mutations in the gene encoding fibrillin-1 (*FBN1*) and characterized by a number of skeletal abnormalities, aortic root dilatation and sometimes ectopia lentis (Robinson et al., 2006). Although the molecular pathogenesis of MFS was attributed initially to a structural weakness of the fibrillin-rich microfibrils within the ECM, more recent results have documented that many of the pathogenic abnormalities in MFS are the result of alterations in TGF-β signaling (Habashi et al., 2006; Neptune et al., 2003; Ng, 2008). Mutations in the genes encoding the TGF-β receptors type I and II (*TGFBR1*, *TGFBR2*) were shown to be associated with a number of diseases with significant clinical similarity to Marfan syndrome (Loeys et al., 2005; Loeys et al., 2006; Mizuguchi et al., 2004; Pannu et al., 2005). Although, for the most part, no strict genotype–phenotype correlations have emerged, important clinical differences have been associated with different *TGFBR2* mutations, suggesting the possibility of distinct biochemical effects of the various mutations. A four-generation family was found to segregate thoracic aortic aneurysms and dissections (TAAD2) in an autosomal-dominant manner. No signs of dural ectasia or ectopia lentis were present but, three out of six patients had a high-arched palate, and two had either pectus deformities or arachnodactyly. No family member displayed a combination of skeletal manifestations characteristic of MFS (Hasham et al., 2003). Subsequently, a mutation in the gene encoding *TGFBR2* was identified in the affected members of this family – 1378C>T (R460C). Strikingly, a mutation at residue R460 was identified in four unrelated families with isolated TAAD, suggesting that mutations at this residue might be a ‘hot spot’ for familial TAAD. Affected persons from two unrelated families with R460C mutations presented primarily with dilatation of the ascending aorta or type A dissections. By contrast, affected persons of one of the two families with the mutation R460H mutation presented with both ascending and descending thoracic aortic disease, and some also had carotid and cerebral aneurysms and dissections (Pannu et al., 2005). Subsequent reports on further unrelated probands with

Journal of Cell Science

R460C or R460H confirmed that many affected individuals appeared to have isolated TAAD, but several subjects did have other manifestations characteristic of LDS or MFS, including combinations of multiple skeletal features that fulfilled the major criterion for the skeleton according to the Ghent nosology or tortuosity of the carotid or cerebral arteries (Disabella et al., 2006; Law et al., 2006; Loeys et al., 2006; Singh et al., 2006).

Despite the clinical variability, the clinical phenotype of carriers of the R460H or R460C mutations does seem to be distinct from the phenotype of classical Loeys–Dietz syndrome because features such as bicuspid aortic or pulmonary valve, hypertelorism, bifid uvula and learning disability are rare (Law et al., 2006), although persons with R460H with clear LDS type I or II have been reported (Loeys et al., 2006). Patients from nine unrelated families with the mutations R528C or R528H have been reported to have LDS type I (LeMaire et al., 2007; Loeys et al., 2006). The mutation R537C was reported in a patient diagnosed with Marfan syndrome type II and showing skeletal and cardiovascular manifestations of MFS without typical ocular involvement (Mizuguchi et al., 2004). A subsequent report found the same mutation in an unrelated person with LDS type I (Loeys et al., 2006). R537P has been found in patients with MFS2 and LDS1 (E. Arbustini, personal communication). We additionally investigated the mutations S449F and L308P, each of which has been reported in a person diagnosed with MFS type II (Mizuguchi et al., 2004), as well as Y336N, which has been reported in LDS type I (Loeys et al., 2005).

The fibrillins have an architectural function as a major component of extracellular microfibrils and also regulate mobility and activation of cytokines such as TGF-β1 and bone morphogenetic protein 7 (BMP7) (Chaudhry et al., 2007; Gregory et al., 2005). Secreted TGF-β dimers remain noncovalently bound to their pro-peptides (latency-associated peptide, LAP), which inhibit interaction with TGF-β receptors. LAP in turn is covalently attached to latent TGF-β-binding proteins (LTBP1 and LTBP3) to form the large latent complex (LLC). The LLC is sequestered to the extracellular matrix through binding of LTBP proteins to fibronectin and fibrillin (ten Dijke and Arthur, 2007). Mutations in *FBN1* are therefore associated with increased activity and bioavailability of TGF-β1, which is suspected to be the basis for phenotypical similarities of *FBN1* mutations in Marfan syndrome and mutations in the receptors for TGF-β in Marfan-syndrome-related diseases (Chaudhry et al., 2007).

Upon activation, dimeric TGF-β1 and TGF-β3 bind to homodimers of the TGF-β type II receptor (TβRII). Binding of TGF-β to TβRII allows for recruitment of the type I receptor (TβRI). While TβRII molecules are activated following autophosphorylation by their constitutively active kinase domain, TβRI needs to become transphosphorylated by TβRII at specific serine residues in its glycine–serine-rich (GS-) domain in order to render its kinase active (Wrana et al., 1994). TβRI then phosphorylates the receptor- (R-) Smads, Smad2 and Smad3, at carboxy-terminal serine residues. C-terminal phosphorylation of R-Smads induces association with the Co-Smad Smad 4. These Smad complexes accumulate in the nucleus to regulate transcription in concert with transcription factors and DNA-binding cofactors (Ross and Hill, 2008). TGF-β can also activate additional signaling pathways, including the extracellular-signal-regulated kinases (ERK1 and ERK2) (Lee et al., 2007; Mulder, 2000), p38 mitogen-activated protein kinase (p38-MAPK), c-Jun N-terminal kinase (JNK) (Sorrentino et al., 2008; Yamashita et al., 2008) and phosphoinositide 3-kinase–Akt (PI3K-Akt) (Bakin et al., 2000; Wilkes et al., 2005) pathways through mechanisms not directly involving Smads.

To date, the effects of mutations in the kinase domain of the TGF-β type II receptor that were identified in distinct hereditary diseases have not been correlated with their differential pathologic manifestations. Using a number of quantitative signaling studies, we were able to measure the impact of mutations in TGFBR2 associated with MFS2, LDS and TAAD on TGF-β signaling pathways.

Results

Mutations in the TGF-β receptor II kinase domain

We performed a comprehensive analysis of nine mutations from MFS-related diseases that are located in the core of the TβRII kinase domain (Fig. 1A). As the structure of the TβRII kinase has

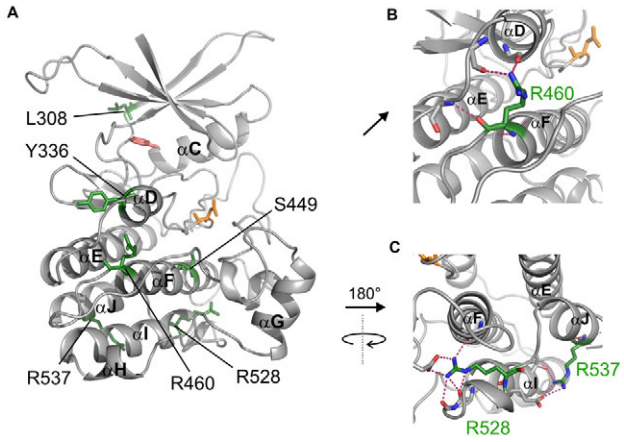

Fig. 1. Mapping of mutations in the kinase domain. (**A**) The nine mutations investigated in this study are shown in a model of the TβRII kinase domain. Except for L308, all mutations investigated map to the lower lobe of the kinase (represented as sticks, green). For orientation, the position of the adenine moiety of ATP (from ActRIIB) and the catalytic aspartate are indicated in red and yellow, respectively. Helix nomenclature was adopted from ActRIIB. (**B**) Detail showing R460 (green) with intramolecular H-bonds (pink, broken line). The arginine residue at position 460 in TβRII RII is located at the C-terminal end of αF. This helix forms the central anchoring element in the architecture of eukaryotic kinases (Kornev et al., 2008). R460 is conserved among all type I and type II receptors of the TGF-β superfamily (supplementary material Fig. S1) and contributes to the stability of the lower C-lobe by forming intramolecular H-bonds to backbone carbonyl oxygen atoms in αD (Borders et al., 1994) and the downstream loop. (**C**) R528 and R537C [after 180° rotation of (A)]. R528 is positioned between the αI and αJ in the lowermost part of the kinase, and this residue is conserved in all TGF-β superfamily receptors (supplementary material Fig. S1). On the basis of homology to ActRIIB, both R528 and R537 are predicted to form hydrogen bonds to backbone carbonyls as well as salt bridges to conserved glutamate residues, which presumably is important for the stabilization of the kinase domain. The R528 side-chain forms multiple H-bonds to backbone carbonyls, and, in addition, a salt bridge with E428. This glutamic acid residue is conserved throughout the family, and the salt bridge is present in all TGF-β superfamily receptor kinase structures available to date (ActRIIB, Alk2, Alk5, BMPR2). R537 is situated in αJ at the far side of the substrate-binding pocket and on the solvent surface. The arginine side-chain H-bonds to T516 and forms a salt bridge to E519 in the neighboring αI. These bonds are present in TβRII and ActRIIB; however, no such bonds are present in the structures of Alk2, Alk5 or BMPR2. In the type I receptors, the arginine is replaced by a threonine residue, whereas, in BMPR2, which has an arginine at this position, αI-glutamate is exchanged to the smaller aspartate (supplementary material Fig. S1).

not been published to date, we generated a model based on the structure of the highly homologous activin receptor type IIB (ActRIIB) kinase domain (Han et al., 2007) using SWISS-MODEL (Arnold et al., 2006; Guex and Peitsch, 1997; Schwede et al., 2003).

L308 is located at the beginning of beta-sheet 4 (β4), Y336 in α-helix D (αD) and S449 in αF (Fig. 1A). Arginine residues R460, R528 and R537 are highly conserved residues in the TGF-β receptor family (supplementary material Fig. S1), and they contribute to preserving the kinase structure by a series of intramolecular polar interactions (Fig. 1B,C). Mutations of these residues are therefore very likely to alter the arrangement of the kinase structure and will potentially compromise kinase activity. In addition, R460 maps close to the substrate-interacting regions. Mutations of R460 might thus directly affect substrate binding.

Expression and turnover of mutant receptors

Mutations were introduced in TβRII wild-type expression constructs. Two sets of receptor mutants were generated, comprising either an N-terminal HA-tag or a FLAG-tag at the C-terminus. Expression of the receptors was verified by western blot from total lysates of transfected COS7 cells (Fig. 2A). Significant differences in receptor expression were found for all mutations when compared with wild-type receptors. Both the 70-kDa unglycosylated TRβII, which represents the immature receptor in the endoplasmic reticulum (ER), and the glycosylated forms of ~90 kDa, representing the cell surface form of TβRII (Wells et al., 1997), were markedly reduced for all mutations when compared with the wild-type receptor (Fig. 2A). Quantitative RT-PCR confirmed that reduced expression is a consequence of these mutations at the protein level rather than an artefact of plasmid quality as all mutated receptor mRNAs are present at levels comparable to those of the wild-type receptor (supplementary material Fig. S2). Receptors with mutations Y336N and S449F were barely expressed and are likely to lead to haploinsufficiency for TβRII. For the subsequent analysis, we focused on mutations of conserved arginines R460, R528 and R537.

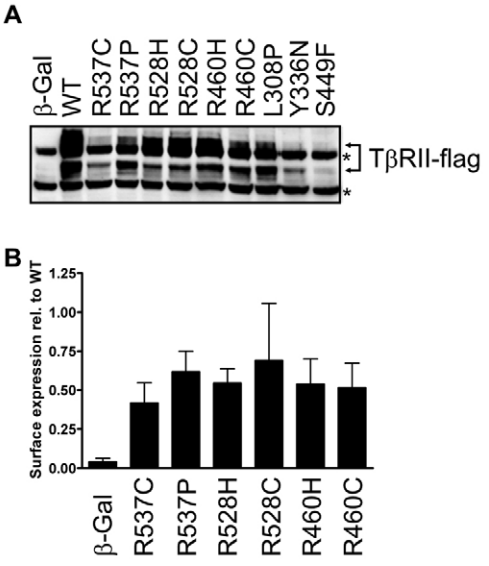

Fig. 2. Expression of TβRII mutants. (**A**) Western blot analysis of lysates from COS7 cells transfected with wild-type (WT) or mutants of TβRII, or control (β-galactosidase); asterisks (*) identify nonspecific bands of the antibody against FLAG. (**B**) Levels of surface expression of TβRII kinase mutants relative to wild-type controls after transfection into HEK293T cells. Epitope-tagged TβRII was stained on nonpermeabilized cells, and mean fluorescence intensity values were compared with those of wild-type controls (WT=1). Error bars represent the s.d. of three independent experiments.

To determine the actual amount of mutated TβRII at the plasma membrane, N-terminally HA-tagged receptors were overexpressed in HEK293T cells and quantified by flow cytometry on nonpermeabilized cells. Surface expression, as determined by mean fluorescence intensity, is reduced for all mutations investigated, ranging from 40% for R537C to 75% for R528C in comparison with WT-TβRII (Fig. 2B). Mutations of single amino acids in the kinase domain of TβRII markedly affect expression and membrane localization of these receptors. However, it could be shown that all mutant receptor variants that were subject to further characterization are targeted to the plasma membrane at significant levels.

To investigate whether TβRII mutations also affect receptor internalization, we transfected HEK293T cells with HA-tagged receptors. After labelling of surface TβRII at 4°C with primary antibodies, cells were shifted to 37°C to allow for receptor internalization for different periods of time. Labelled receptors remaining on the cell surface were then visualized with fluorescent secondary antibodies. Constitutive receptor endocytosis is represented by the decrease of surface fluorescence with internalization time. We observed 40% and 60% of wild-type TβRII being internalized after 15 and 45 minutes, respectively (Fig. 3). The endocytosis rate, determined from the linear part of the internalization curve, was 0.025 $minute^{-1}$. Both values match those published for TβRII (Ehrlich et al., 2001). Receptor internalization could be blocked by the dynamin GTPase inhibitor dynasore at 160 μM (Fig. 3G) (Macia et al., 2006). A mutant TβRII in which a di-leucine motif is mutated showed greatly reduced internalization, as expected (Fig. 3H) (Ehrlich et al., 2001). Endocytosis of R537C, R537P, R528H and R460C was mildly attenuated in comparison with WT-TβRII but did not differ significantly (Fig. 3A–C,F), whereas R528C underwent endocytosis at a rate that was not distinguishable from that of the WT-TβRII (Fig. 3D). Internalization of R460H, however was severely compromised as only 15% and 30% of the receptors internalized after 15 and 45 minutes, respectively (Fig. 3E).

Taken together, we found that, as a consequence of various mutations in the TβRII kinase domain, receptor turnover, including expression, posttranslational processing, trafficking to the surface and receptor internalization, are affected differentially, depending on the site and nature of the mutation.

Autokinase activity of mutated receptors

We next analyzed whether the enzymatic activity of the TβRII kinase is compromised by these mutations. HEK293T cells were transfected with FLAG-tagged receptor constructs. Overexpressed receptors were immunoprecipitated and subjected to an in vitro kinase assay using radioactively labeled [γ-^{32}P]ATP to visualize autophosphorylation of TβRII (Fig. 4A). Phosphorylated wild-type TβRII was detected in the autoradiogram at approximately 76 and 95 kDa. By contrast, none of the mutant TβRII displayed significant autokinase activity in vitro.

Reporter gene activation by TβRII mutants

A series of experiments was performed to investigate the consequence of these mutations on TGF-β signal transduction. The 3TP-luciferase reporter contains a fragment from the human

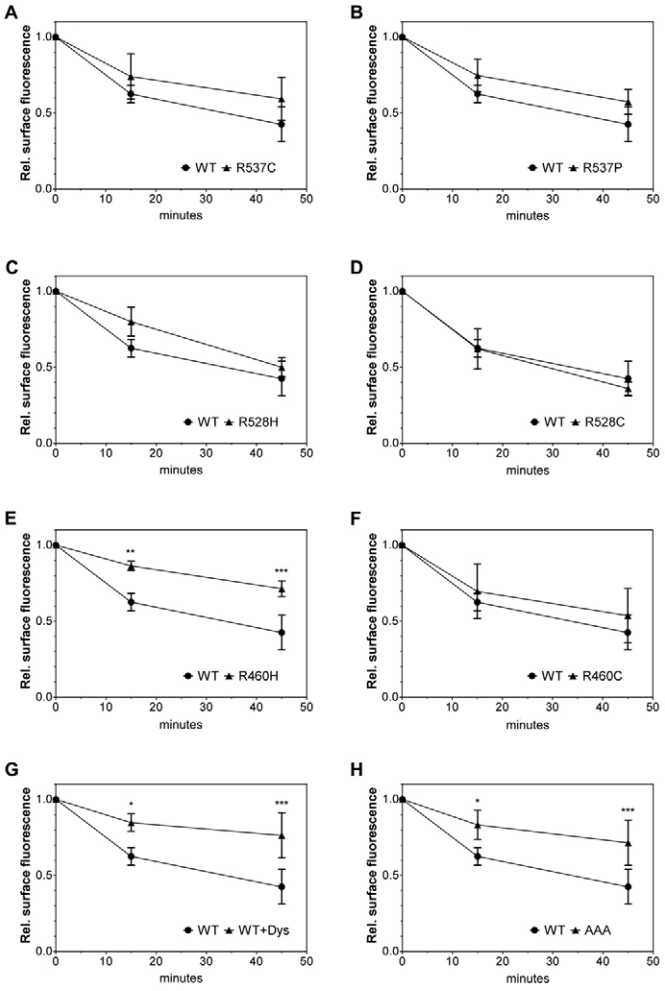

Fig. 3. Receptor endocytosis in HEK293T cells. Cells were transfected with HA-tagged wild-type (WT) TβRII or mutated versions. Cell surface receptors were labeled with an HA-tag-specific antibody. After internalization of the labeled receptor at 37°C, antibody–receptor complexes remaining on the cell surface were recognized by fluorescent secondary antibodies and quantified using flow cytometry. Surface fluorescence of WT-TβRII-transfected cells was decreased by 40% after 15 minutes of incubation at 37°C, and, after 45 minutes, 60% of receptors had been endocytosed. Internalization was slightly attenuated for R537C and R537P (**A**,**B**), R528H (**C**), R460C (**F**), whereas R528C (**D**) internalizes like WT-TβRII. Internalization of R460H (**E**) was reduced substantially and was comparable to WT-TβRII treated with dynasore (Dys) (**G**) and an internalization-defective TβRII mutant (AAA) (**H**). Data are shown as means of relative (±s.d.) median fluorescence intensities from three independent experiments. Asterisks indicate statistical significance (two-way ANOVA followed by Bonferroni's post test for multiple comparisons): **P*≤0.05; ***P*≤0.01; ****P*≤0.001.

plasminogen activator inhibitor 1 (PAI1) promoter following three 12-*O*-tetradecanoylphorbol-13-acetate (TPA) response elements (Wrana et al., 1992). Responsiveness of the 3TP-luc reporter was shown to be promoted by non-Smad TGF-β-induced JNK or ERK MAPK activity in addition to Smad signaling (Carcamo et al., 1995; Sirard et al., 2000).

In initial experiments, the effect of TβRII mutations on endogenous TGF-β signaling was monitored by transfecting wild-type or mutated receptors into HEK293T cells (Fig. 4B). Transfection of kinase-deficient LDS mutation R528C repressed the 3TP-luciferase response to the same amount as a dominant-negative truncation of TβRII that lacks most of the cytoplasmic domain (TβRII-ΔCyt) (Wieser et al., 1993), suggesting a dominant-negative effect of R528C. Subcellular fractionation (supplementary material Fig. S3A) and immunocytochemistry (supplementary material Fig. S3B) to visualize Smad2 phosphorylation and nuclear translocation further confirmed our findings that R528C is an inactive receptor mutant that represses the TGF-β pathway in a dominant-negative manner.

For further scrutinization of signaling activity, we performed experiments in DR26 mink lung epithelial cells. DR26 cells lack expression of endogenous TβRII (Wrana et al., 1992) and thus provide a system that allows the control of the ratios between wild-type and mutated receptors by titrating transfected constructs. These cells are well-established systems for functional assays in the TGF-β field but are less suitable for flow cytometry measurements of receptor surface expression or internalization as they adhere strongly to the growth surface and have to be detached by enzymatic digestion, which tends to affect surface antigens.

Cells were transfected with various amounts of wild-type TβRII plasmid, ranging from 100% of total plasmid to 0%, which was complemented to 100% with plasmid DNA coding for receptor mutations or control plasmids. As in all the following experiments of this type, the total amount of transfected DNA was kept constant to avoid overloading of the expression or signaling machinery. Activity of the 3TP-luc reporter only marginally decreased with diminished amounts of TβRII plasmid if empty vector, GFP or receptor tyrosine kinase-like orphan receptor 2 (Ror2) were used as complement. Ror2, which is a transmembrane receptor tyrosine kinase, was expressed under the same promoter (CMV) as our receptor constructs and served as an internal control showing that coexpression of an unrelated surface receptor does not interfere with TβRII signaling. Strikingly, with as little as 25% of the total DNA being wild-type, the response was still approximately 75% of the wild-type-only signal (Fig. 4C) in all controls. By contrast, titration with R528C repressed the reporter signal in a dominant-negative fashion (Fig. 4C).

This finding strongly supports the conclusion that, in our experimental setup, the effect of a dominant-negative mutation becomes manifest in an approximately linear function of reporter gene activity, which decreases with increasing coexpression of a dominant-negative receptor. We now performed DNA titration reporter gene assays for mutations associated with MFS2 (R537C, R460H), LDS (R537P, R528H and R528C) and TAAD (R460C) using 3TP and $(CAGA)_{12}$ luciferase reporter constructs (Fig. 5). In order to dissect the impact on both Smad and non-Smad signaling, two different reporter gene constructs were used. While the 3TP-luc reporter reads both Smad and non-Smad TGF-β signaling, as mentioned above, the $(CAGA)_{12}$-luc reporter contains 12 Smad-binding elements (SBEs) that bind active Smad3–Smad4 complexes; thus, it is activated directly by active TGF-β–Smad signaling only (Dennler et al., 1998). For mutations of R537, a dominant-negative effect manifested on the 3TP-luc and $(CAGA)_{12}$-luc reporter (Fig. 5A–D). Interestingly, the dominant-negative effect of R537P was more potent than that of R537C, leading to a more-than-linear decline of signal intensity with decreasing portions of transfected WT-TβRII (Fig. 5B,D). Both mutations were incapable of mediating any TGF-β response in the absence of wild-type receptor molecules. The latter finding held true also for mutations of arginine at position 528 (R528H and R528C), which were shown to be inactive on both 3TP-luc and $(CAGA)_{12}$-luc

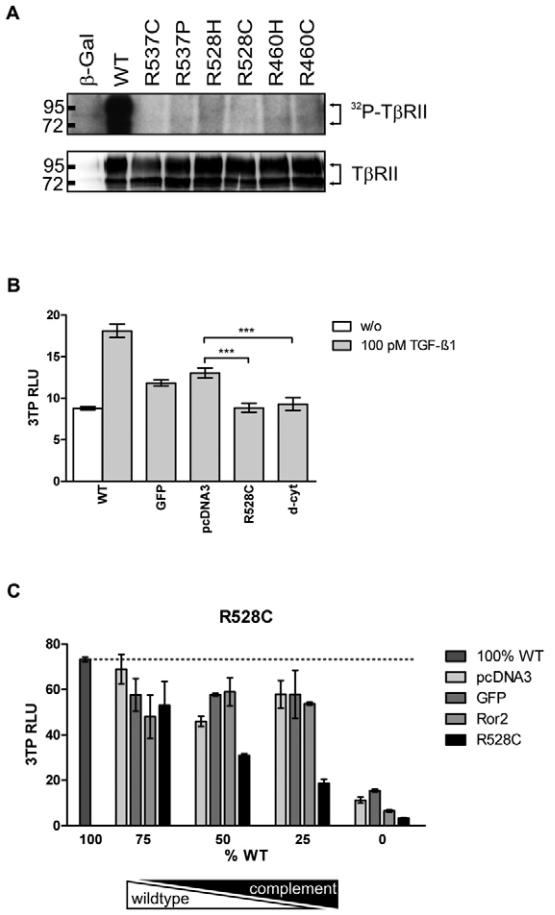

Fig. 4. Effect of dominant-negative mutations of TβRII on kinase function and reporter gene activity. (**A**) Kinase activity of mutated TβRII. FLAG-tagged TβRII receptors were immunoprecipitated and subject to an in vitro kinase reaction with [γ-^{32}P]ATP. The autoradiogram shows ^{32}P-phosphorylated TβRII (upper panel, arrows), and the western blot (lower panel) indicates the amount of total TβRII in the immunoprecipitates. (**B**) TGF-β-induced response on the 3TP-luc reporter in HEK293T cells after transfection with wild-type or mutated receptors, including a dominant-negative TβRII lacking most of the cytoplasmic domain (d-cyt) or controls (GFP, pcDNA3). Error bars represent the s.d. from triplicate measurements; asterisks indicate statistical significance (one-way ANOVA followed by Tukey's multiple comparison test): ***$P \leq 0.001$. (**C**) Response from 3TP-luc reporter in DR26 cells transfected with increasing ratios of mutated (R528C) or control complement DNA versus wild-type TβRII constructs; cells were stimulated with 100 pM TGF-β1; error bars represent the s.d. from triplicate measurements. RLU, relative luminescence units (3TP-luc/RLTK-luc).

reporters (Fig. 5E–H). In addition, as shown before in HEK293T and DR26 cells for R528C (Fig. 4B,C), receptors carrying these mutations interfere with the activation of signaling by wild-type molecules in a dominant-negative manner. The dominant-negative potential of both mutants, however, was largely the same for R528C and R528H.

Finally, mutations of R460 to histidine (R460H) or cysteine (R460C), which have been found in MFS2/LDS and TAAD, respectively, were characterized using the same strategy. The R460H mutation also showed a dominant-negative behavior in the absence of residual activity on any reporter (Fig. 5I,K). By contrast, a cysteine in this position did not entirely abolish the responsiveness to TGF-β (Fig. 5J,L). This mutant retained some residual signaling activity even in the absence of WT-TβRII and thus exhibited only a weak dominant-negative effect on the signaling activity of wild-type TβRII on the Smad3–Smad4-dependent $(CAGA)_{12}$-luciferase reporter. On the 3TP-luc promoter that integrates both Smad and non-Smad pathways, R460C alone had only marginal activity, and the dominant-negative effect was more pronounced (Fig. 5J).

Taken together, all but one mutant TβRII were shown to interfere with transcriptional activity of TGF-β signaling in a dominant-negative fashion. The TAAD mutation R460C was able to induce TGF-β signaling on both promoters to some extent. These findings prompted a more detailed investigation of TGF-β-induced signaling in order to dissect the Smad and non-Smad signaling activities of these mutations. In addition, we tested mutations L308P, Y336N and S449F in the absence of WT-TβRII and found that they were inactive (supplementary material Fig. S4).

Activation of Smad pathways and non-Smad pathways

We next sought to determine the ability of TβRII mutations to mediate Smad2 phosphorylation. DR26 cells were again transfected with receptor constructs, and Smad2 phosphorylation was determined after short-term stimulation. Although wild-type TβRII reconstituted phosphorylation of Smad2 after 5 to 40 minutes stimulation with TGF-β1, neither of the mutations investigated was able to do so to a similar extent (Fig. 6A,B). After 15 and 40 minutes of stimulation, however, R460C induced some phosphorylation of Smad2, suggesting that this mutation did not entirely demolish Smad activation. This correlates with our findings in reporter gene assays (Fig. 5J,L).

TGF-β is able to induce directly activation of non-Smad signaling such as ERK and p38 MAPK pathways in most cells types (Zhang, 2009). Activation of ERK could be measured after 40 minutes of TGF-β stimulation if wild-type TβRII was introduced, whereas all mutations annihilated TGF-β-induced activation of ERK (Fig. 6A,B) in DR26 cells. In summary, only the R460C TAAD mutant was able to induce Smad activation to some extent, whereas none of the TβRII mutants displayed ERK signaling activity.

Discussion

TGFBR mutations in MFS and related diseases

Mutations in the genes encoding TGF-β receptors I and II (*TGFBR1*, *TGFBR2*) have been found in patients with a range of clinical presentations (Loeys et al., 2006). At the mild end of the clinical spectrum, mutations at the arginine residue at position 460 of *TGFBR2* have been associated with familial thoracic aortic aneurysms and dissections (TAAD) with no or only mild and nonspecific skeletal manifestations (Hasham et al., 2003; Pannu et al., 2005). Several groups have identified *TGFBR2* mutations in patients with with MFS2, which is characterized by thoracic aortic aneurysms or dissections and skeletal abnormalities commonly found in Marfan syndrome, but without ectopia lentis, which is an ocular finding with high specificity for classic MFS (Disabella et al., 2006; Mizuguchi et al., 2004; Singh et al., 2006). Loeys–Dietz syndrome represents the severe end of the spectrum. In addition to the above findings, affected patients can display hypertelorism, bifid uvula, cleft palate and generalized arterial tortuosity with widespread vascular aneurysms and dissections (Loeys et al., 2005). A subset of patients additionally co-presents with features characteristic of the vascular type of Ehlers–Danlos syndrome such as vascular rupture, uterine, splenic or intestinal rupture, translucent

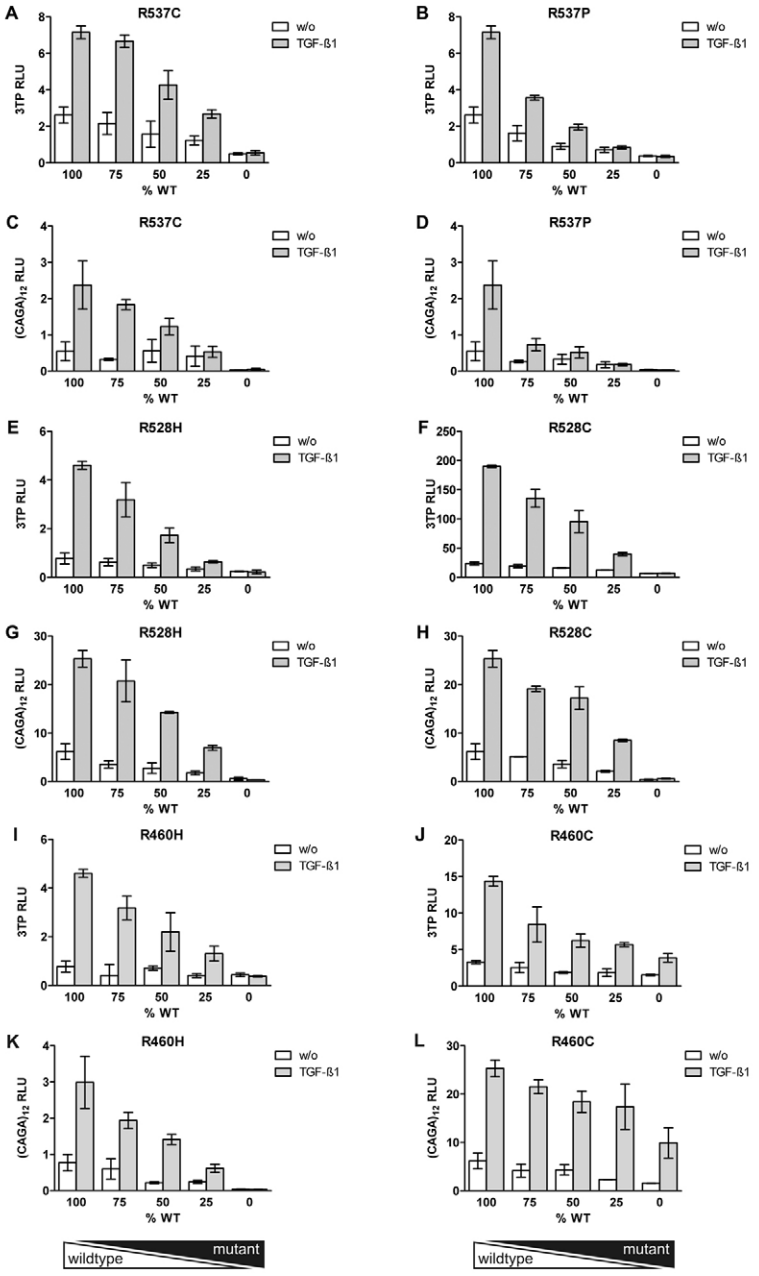

Fig. 5. Induction of 3TP-luc and (CAGA)12-luc reporters after titration of wild-type (WT) versus mutated plasmids in DR26 cells. Cells were transfected with decreasing amounts of WT plasmid, complemented to 100% with the mutated construct. (**A–D**) Dominant-negative effect of R537 mutations on the 3TP-luc reporter construct (A,B) as well as on a $(CAGA)_{12}$-luc reporter, as indicated by a roughly linear decrease of the luminescent signal. (**E–H**) Mutations of R528 exhibited a dominant-negative effect on the 3TP and $(CAGA)_{12}$-luc luciferase reporter gene. (**I–L**) 3TP-luc and $(CAGA)_{12}$-luc reporter activity in DNA titration experiments introducing R460H and R460C. (I,K) R460H had a dominant-negative effect on the TGF-β signal both on 3TP-luc and $(CAGA)_{12}$-luc reporters. (J,L) The R460C mutation affected 3TP-luc reporter activity in a dominant-negative manner; when this mutation was expressed in the absence of wild-type TβRII, it revealed residual activity. On the $(CAGA)_{12}$-luc reporter, the dominant-negative effect was less pronounced, and the mutated receptor was able to induce significant reporter activity. Error bars represent the s.d. from triplicate measurements. RLU: relative luminescence units (3TP-luc/RLTK-luc or $(CAGA)_{12}$-luc/RLTK-luc).

skin and atrophic scars (Loeys et al., 2006). The latter presentation has been termed Loeys–Dietz syndrome type 2.

There has long been a debate in human genetics between the ‘lumpers’ and the ‘splitters’ (McKusick, 1969). For Loeys–Dietz syndrome, the question is whether it is sensible to draw lines in the phenotypic spectrum between persons with predominantly aortic abnormalities (TAAD), those with aortic abnormalities as well as skeletal abnormalities characteristic of Marfan syndrome (MFS2) and those with additional features of full-blown Loeys–Dietz syndrome, including craniofacial abnormalities such as craniosynostosis. If one accepts the ‘splitter’ viewpoint, one can say that the clinical features of TAAD represent a subset of the features of Marfan syndrome type 2, which in turn represent a subset of the features found in severe Loeys–Dietz syndrome (Fig. 7).

That said, it must also be mentioned that clinical reality is not as simple as might be suggested by Fig. 7. There is a high degree of clinical heterogeneity in persons with mutations in *TGFBR2* (Attias et al., 2009). As described in detail in the introduction, carriers of the mutation R460C have been described as having TAAD or LDS by several different groups. In addition to TAAD, there has been a convincing report of a patient with the mutation R460C in whom the diagnosis MFS2 was made after features of classical LDS such as uvula bifida, craniofacial signs of LDS and arterial tortuosity had been ruled out (Singh et al., 2006).

Thus, there is no strict genotype–phenotype correlation for *TGFBR2* mutations. Different patients with the same mutation can have different phenotypes. For instance, the mutation R460H has been reported in persons diagnosed with TAAD, MFS2, LDS1 and LDS2 (Table 1). Presumably, this phenotypic variability could be due to the influence of modifying genes or environmental factors. In some cases, the specific diagnosis made could reflect ascertainment bias related to the phenotyping practices of individual clinical centers.

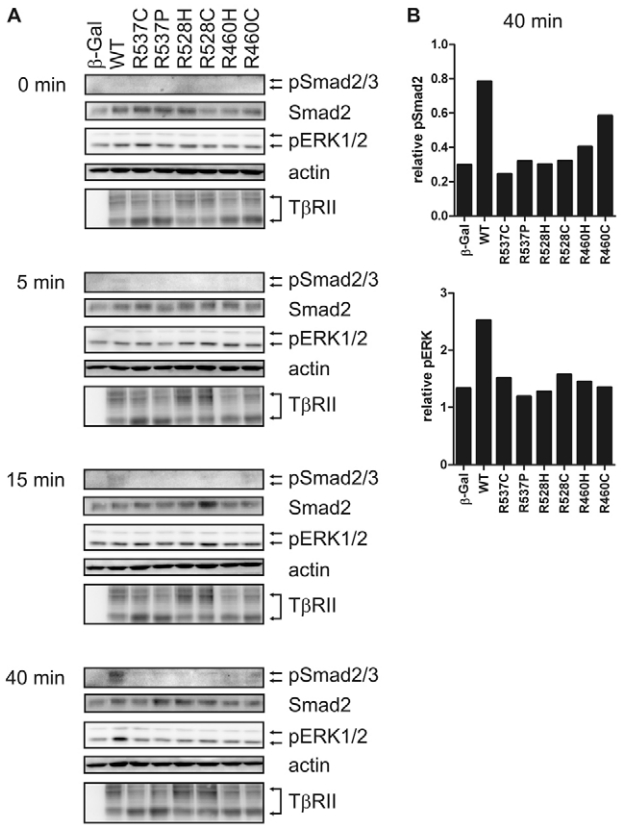

Fig. 6. Activation of Smad and ERK pathways by TβRII mutations. DR26 cells were transfected with wild-type (WT) TβRII or mutated receptors. (**A**) Following starvation, cells were stimulated with TGF-β1 for different periods of time. Only R460C and, even more weakly, R460H mutations mediated residual Smad phosphorylation, but none of the mutated receptors was capable of inducing phosphorylation of extracellular-signal-regulated kinases 1 and 2 (ERK1/2) after TGF-β stimulation. (**B**) Quantification of phospho-Smad2 and ERK1/2 signals from western blot after 40 minutes of stimulation. Relative pSmad2 and pERK intensities were obtained by normalizing to total Smad2.

This represents a limitation of our study and should be taken into account in the interpretation of potential clinical correlations of the biochemical findings reported in this work. Nonetheless, we contend that the bulk of the clinical evidence suggests that mutations at R460 tend to be associated with relatively mild phenotypes that in many cases can be adequately described by the term TAAD.

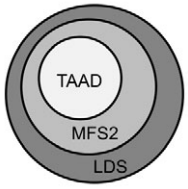

Fig. 7. The clinical manifestations of familial thoracic aortic aneurysm and dissections (TAAD), Marfan syndrome type 2 (MFS2) and Loeys–Dietz syndrome (LDS). TAAD is characterized by thoracic aortic aneurysm or dissections with or without mild and nonspecific skeletal findings. MFS2 is additionally characterized by skeletal findings typical of those found in classical MFS due to mutations in *FBN1*. LDS is characterized by all of these findings as well as additional dysmorphic features, generalized arterial tortuosity and, in some cases, mild mental retardation.

Differential expression and turnover of mutant TGF-β receptors

In this study, we aimed to characterize the biochemical features of a series of mutations associated with MFS2, LDS and TAAD by characterizing their signaling properties quantitatively in well-established TGF-β signaling assays and correlating them to their clinical phenotypes. Expression of all mutants was markedly reduced in comparison with wild-type expression in total cell lysates. Both the unglycosylated ER form of the receptor and glycosylated mature receptors were less abundant, with the strongest defects affecting Y336N and S449F. These mutants were therefore not subjected to further investigation. We subsequently focused on mutations of the conserved arginine residues R460, R528 and R537. Flow cytometric analysis of transmembrane TβRII revealed that, except for R528H, all receptors were expressed on the cell surface at levels of approximately 50% in comparison with wild-type TβRII. R528H showed highly variable expression on the cell surface, which in some experiments was comparable to that of the wild-type receptor. These data emphasize that the mutations that were characterized strongly interfered with receptor folding, processing and/or trafficking.

Quantification of receptor internalization by flow cytometry is widely used on receptor tyrosine kinases and G-protein-coupled receptors (Barak et al., 1994; Wang et al., 2005). In this study, we used a refined experimental procedure to extend its applicability to TGF-β receptors. Most importantly, by excluding apoptotic and necrotic cells as well as cell aggregates using scatter gating and propidium iodide staining of permeable cells, we could greatly improve experimental reproducibility. Our measurements of

Table 1. Reported clinical phenotypes of patients with the *TGFBR2* mutations studied in this work

Mutation	TAAD	MFS2	LDS1	LDS2	References
L308P	0	1	0	0	Mizuguchi et al., 2004
Y336N	0	0	1	0	Loeys et al., 2005
S449F	0	2	0	1	Loeys et al., 2006; Mizuguchi et al., 2004
R460C	16	4	0	0	Hasham et al., 2003; Pannu et al., 2005; Singh et al., 2006
R460H	29	3	23	1	Disabella et al., 2006; Law et al., 2006; Loeys et al., 2006; Pannu et al., 2005
R528C	0	0	4	0	LeMaire et al., 2007; Loeys et al., 2005; Loeys et al., 2006
R528H	0	0	6	0	Loeys et al., 2005; Loeys et al., 2006
R537C	0	9	1	0	Loeys et al., 2006; Mizuguchi et al., 2004
R537P	0	1	1	0	E. Arbustini, personal communication

TAAD, familial thoracic aortic aneurysm and dissections with no or only mild skeletal features (Pannu et al., 2005); MFS2, aortic and skeletal features resembling those of classic Marfan syndrome without ectopia lentis and without other clinical features specific for LDS (Mizuguchi et al., 2004); LDS1 and LDS2, Loeys–Dietz syndrome types I and II.

constitutive receptor internalization as part of signaling and receptor turnover confirmed that the kinase activity of TβRII is not per se a prerequisite for internalization. As reported, TβRII endocytosis is barely affected even by the absence of the entire kinase domain (Ehrlich et al., 2001). By contrast, our data suggest that distinct structural alterations in the kinase can interfere with proper internalization, as shown for R460H. Specifically, the structure surrounding R460 is supposed to be involved in substrate binding and positioning, as is the case for other protein kinases (Kornev and Taylor, 2010), whereas R528 and R537 are at the backside of the lower kinase lobe. Of all mutations investigated in this study, R460 mutations might affect substrate interaction most directly, suggesting that binding of TβRI as the TβRII substrate is a prerequisite for efficient endocytosis of the receptor complex. Alternatively, mutations of R460 might alter the interaction of TβRII with receptor-binding proteins other than TβRI. This will be the subject of further investigation. For instance, it thus appears highly promising to compare the differential interactomes of TβRII-R460 and WT-TβRII to identify differences in protein interaction partners.

TGF-β pathway activity of TβRII mutants

With respect to the fact that mutant receptor expression is decreased significantly in comparison with WT-TβRII, it was crucial to control expression of these mutants by titrating mutant and wild-type DNAs in the absence of endogenous TβRII background. Experiments to calibrate our setup revealed that linear reduction of wild-type receptor DNA did not, as expected, generate a linear decrease in reporter activity. Of note, the cellular response decreased only marginally, and as little as 25% of wild-type receptor DNA was sufficient to generate a response of ~75% in comparison with 100% from the wild-type construct if empty vector, GFP or, most importantly, the receptor tyrosine kinase Ror2 were used as complement. This phenomenon was not considered in previous experiments, which had led to the conclusion that *TGFBR2* mutations in MFS2 do not have a dominant-negative effect (Mizuguchi et al., 2004). By contrast, co-transfection with mutant receptors repressed reporter gene activity, resulting in a linear decrease of the signal. Our data revealed that mutations of R537 and R528 exhibit dominant-negative – rather than simply nonfunctional – effects on both reporters while being incapable of establishing any residual reporter activity if transfected in the absence of wild-type TβRII. Similar results were obtained for R460H. By contrast, R460C was able to generate a significant response on both the $(CAGA)_{12}$ and the 3TP luciferase reporter. Accordingly, all mutated receptors except for R460C were inefficient in inducing Smad phosphorylation in DR26 cells. By contrast, confirming our results from luciferase reporter gene assays, R460C was able to promote weak phosphorylation of Smad2.

Activation of the $(CAGA)_{12}$ reporter was shown to be dependent exclusively on activated Smad3–Smad4 complexes in the nucleus, whereas, owing to the presence of three TPA response elements, the 3TP reporter can be coactivated to some extent by non-Smad TGF-β pathways, such as JNK or ERK–MAPK signaling (Carcamo et al., 1995; Dennler et al., 1998). R460C, like all other mutations investigated, failed to induce ERK phosphorylation after TGF-β stimulation. This might explain our finding that R460C is surprisingly active in inducing the Smad-only response on $(CAGA)_{12}$-luc, whereas its ability to induce 3TP-luc is more strongly affected owing to the missing ERK-activating component.

The TβRII cytoplasmic domain contains a constitutively active kinase and is autophosphorylated at serine, threonine and tyrosine residues (Lawler et al., 1997; Luo and Lodish, 1997). Activating autophosphorylation that occurs in *cis* (intramolecular autophosphorylation within the same polypeptide chain) and *trans* (intermolecular phosphorylation within the TβRII homodimer) promotes full activation of kinase activity and is a prerequisite for TβRII to mediate efficiently the TGF-β signal by transphosphorylating TβRI (Luo and Lodish, 1997; Wrana et al., 1994). Our finding that all mutations of R460, R528 and R537 tested in this study are deficient in in vitro kinase assays with immunoprecipitated receptors suggests that these amino acid exchanges induce rearrangements in the TβRII kinase that render it inactive. Of interest, even R460C, which showed significant signaling activity both in TGF-β reporter gene assays and in Smad phosphorylation assays, turned out to possess, at best, trace activity in this assay. This supports the assumption of a destabilizing effect of R460C that could possibly be compensated by a more favorable environment in our cell-based assays, where decreased receptor mobility in the membrane and associated proteins might stabilize both substrate interaction and kinase structure and enable weak, but significant, signaling activity of R460C.

Residual signaling activity by R460C

R460 maps to the C-terminus of α-helix F in the kinase domain, which was identified as the major structural component in the eukaryotic kinase architecture. αF serves as a scaffold that establishes correct positioning of catalytic, substrate-binding and substrate residues (Kornev et al., 2008). It has been suggested that mutations of R460 affecting the key C-lobe helices perturb *TGFBR2* signaling (Pannu et al., 2005). The discrepancy between the effects of R460H and R460C established in the present study can be explained by analysis of the structural consequences occurring when this residue is mutated (Fig. 8). The side-chain of R460 in TβRII forms two H-bonds to backbone carbonyls in αD and a few residues downstream of αD (Fig. 1B). A histidine side-chain in this position is not able to form these H-bonds but creates steric clashes with the surrounding structure (Fig. 8A). This would induce structural displacements that propagate through the lower C-lobe and might not only disrupt the active kinase structure but also interfere with substrate binding. Mutation of this arginine to cysteine by contrast abolishes intramolecular H-bonds of the arginine side-chain, which presumably leads to structural destabilization of this region (Fig. 8B). The unsaturated H-bonds are close to the solvent surface and thus can be substituted by water molecules. The small cysteine side-chain, however, fits easily into that position, probably without interfering with other structures (Fig. 8B). The distinct consequences of the two mutations fell in line with the predicted change of protein stability induced by R460H or R460C mutations, respectively, calculated using the Eris protein stability prediction server (Yin et al., 2007). Histidine in position 460 has a strong destabilizing effect, as reflected by a positive change in free energy (ΔΔG) in the structures of TβRII, ActRIIB as well as of BMPR2, whereas the destabilization induced by cysteine is less severe in ActRIIB and BMPR2 and is even negligible in our model of TβRII (Fig. 8C).

Thus, although R460H might result in a distorted kinase structure entirely incapable of binding to its substrate and/or to catalyze phosphotransfer, R460C might cause destabilization of the kinase structure, which can be compensated to some extent by binding of

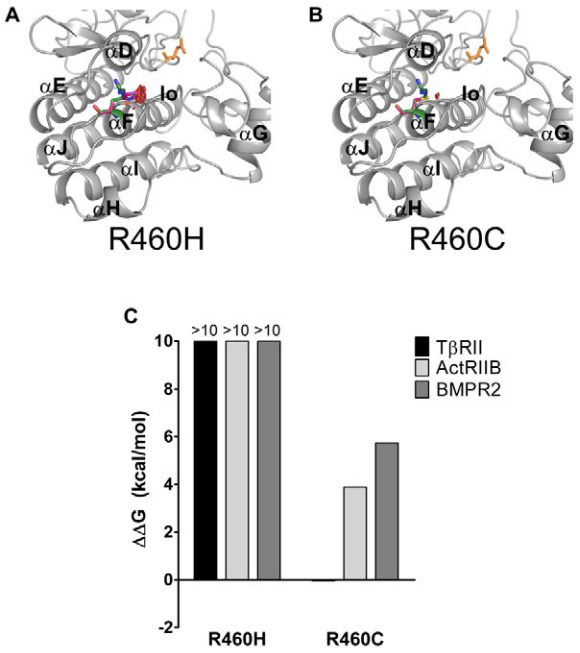

Fig. 8. TβRII kinase structure with mutants of R460. (**A**) R460 (green) is located in the substrate-binding region at the C-terminal end of αF in TβRII. A histidine side-chain (pink) in this position generates severe steric clashes (red discs) with the surrounding structure, especially the lobe preceding αG (lo) that will lead to displacements in the lower lobe of the kinase. (**B**) Cysteine fits in position 460, creating only minor steric incompatibilities. (**C**) Difference in free energy (ΔΔG) representing the change of protein stability induced by mutations of R460, in the structures of TβRII, ActRIIB and BMPR2, respectively. Values were calculated using the Eris protein stability prediction server. ΔΔG<0: stabilizing; ΔΔG>0: destabilizing.

the substrate or accessory proteins and thus might result in reduced, but significant, signaling activity.

Correlation of signaling activities with disease phenotypes

The mutations investigated in this study have been identified in patients reported to have TAAD, MFS2 and LDS (Table 1). Although the lack of detailed and comprehensive clinical information in many of the published studies of these disorders makes a direct comparison of phenotypes difficult, the published clinical evidence would suggest that mutations at R460 tend to be associated with milder phenotypes. R460H has been associated with TAAD, MFS2 and milder forms of LDS, and R460C has been described in individuals with TAAD and MFS2. By contrast, R528C and R528H have both been found only in patients diagnosed with LDS. R537C has been described in a family and one unrelated individual with MFS2 as well as one person diagnosed with LDS1. The mutation R537P was found in a mother with MFS2 whose daughter had a typical facial phenotype of LDS1 (E. Arbustini, personal communication). It is tempting to speculate that the different behavior of some of the mutations characterized in this work might be related to the different clinical phenotypes. Specifically, the mutation R460C had the most mild dominant-negative effect and the highest residual TGF-β signaling activity on the Smad pathway, which sets it apart from all other mutations, whereas failure to induce TGF-β-induced ERK activation is a common feature in all the mutations tested. The residual capability to induce Smad signaling thus could be sufficient to suppress the additional phenotypic defects that manifest in LDS and MFS2.

Conclusions

A series of studies has reported paradoxical upregulation of TGF-β signaling in aortic tissues of patients with mutations in the *TGFBR2* kinase domain, as shown by increased levels of nuclear phosphorylated Smad, abundance of TGF-β and expression of TGF-β target genes (Carta et al., 2009; Gomez et al., 2009; Loeys et al., 2005). The basis of this observation, however, has not been elucidated to date. It was speculated that intrinsic features of those mutations such as altered receptor endocytosis or alternative pathways might promote TGF-β–Smad signaling in this scenario (Jones et al., 2008). Our quantitative biochemical and cell-based analyses do not support the assumption of a general cell-autonomous mechanism by which the respective mutant variants of TβRII paradoxically induce elevated TGF-β activity, although our experiments were not designed to investigate the long-term effects of *TGFBR2* mutations on cellular networks related to TGF-β signaling. The most promising way to clarify the phenomenon of paradoxical activation of Smad signaling will therefore be to investigate intercellular communication in affected tissues in detail, such as to identify the cells that secrete TGF-β and those responding to elevated levels of TGF-β. Further ex vivo studies using patient tissues and cells, and, even more promisingly, mouse models for individual MFS-related mutations hopefully will shed light on these important issues in the future.

The present study has documented that different *TGFBR2* mutations have distinct effects on protein stability and localization, receptor turnover and signaling in the Smad and ERK pathways. Many of the mutations demonstrated a striking dominant-negative effect on Smad and ERK signaling. Characteristic cell biological differences between mutations associated with MFS2 and LDS did not emerge in the course of our study (Table 2). However, it is striking that the R460C mutation, which has been associated with TAAD rather than MFS2 or LDS, showed a quite distinct biochemical phenotype, in that, of all tested *TGFBR2* mutants,

Table 2. Quantitative differences of the nine *TGFBR2* mutations studied in this work on several cell biological parameters

Mutation	Pr. ex.	Rec. int.	AK	Dom. neg.	Smad	ERK
L308P	↓↓	ND	ND	ND	ND	ND
Y336N	↓↓↓	ND	ND	ND	ND	ND
S449F	↓↓↓	ND	ND	ND	ND	ND
R460C	↓	↓	↓↓↓	+	↓↓	↓↓↓
R460H	↓	↓↓↓	↓↓↓	++	↓↓↓	↓↓↓
R528C	↓	→	↓↓↓	++	↓↓↓	↓↓↓
R528H	↓	↓	↓↓↓	++	↓↓↓	↓↓↓
R537C	↓↓	↓	↓↓↓	++	↓↓↓	↓↓↓
R537P	↓	↓	↓↓↓	++	↓↓↓	↓↓↓

Pr. ex., protein expression (including both immature form in the ER and membrane-bound mature forms); Rec. int., receptor internalization; AK, autokinase activity of the isolated mutant receptor in vitro; Dom. neg., dominant-negative effect; Smad, ERK, activation of Smad signaling and activation of ERK in luciferase reporter and phosphoprotein assays. ↓, ↓↓ or ↓↓↓ indicate mild, moderate or severe reductions, respectively, in the indicated parameters. → indicates no change compared with wild type (WT). +, ++ or +++ indicate a mild, moderate or severe dominant-negative effect, respectively; ND, not determined.

only R460C possessed residual Smad signaling activity and only a minor degree of dominant-negative effect on wild-type *TGFBR2*. It appears possible that this residual Smad signaling activity is able to prevent the craniofacial and skeletal phenotypic manifestations characteristic of MFS2 and LDS, but that the *TGFBR2* function is still sufficiently disturbed to cause defects in aortic homeostasis that lead to aortic dilatation and dissection. By contrast, it would appear that both near haploinsufficiency due to lack of expression of *TGFBR2* in the cell membrane (as seen with the mutations Y336N and S449F) or dominant-negative effects of *TGFBR2* missense mutations on Smad and ERK signaling (as seen with the mutations R528C, R528H, R537C and R537P, and also R460H) lead to defects in TGF-β signaling sufficiently severe to predispose to the development of phenotypic defects not only in the aorta but also in the other organ systems typically affected by MFS2 and LDS. Alternatively, the fact that the clinical phenotypes of *TGFBR2* mutations that were barely expressed in our study and those that were dominant negative have not been diagnosed differentially might reflect chronic regulatory effects in vivo.

As both R528C and R528H have been associated with LDS (Table 2), it would appear that the difference in receptor turnover observed for the two mutants (Fig. 3) is not necessarily associated with phenotypic differences.

Materials and Methods

Generation of TβRII expression constructs and quantitative RT-PCR

The coding sequence of TβRII with N-terminal HA-tag, or a FLAG-tag at the C-terminus, was excised from its source plasmid pcDNA1 using *Not*I and *Bam*HI and subcloned to the pcDNA3.1 vector. Mutant constructs were generated using the GeneTailor Site-Directed Mutagenesis kit (Invitrogen). The primers used are listed in supplementary material Table S1. Plasmids were purified using the Promega Mini kit (Promega) and verified by DNA sequencing. RNA preparation was achieved using the TotalRNA Kit (Peqlab) according to the manufacturer's protocols. Reverse transcription was performed using MMLV reverse transcriptase (Promega) and anchored NV-oligo-dT primers (Invitrogen). SYBR-Green qPCR was performed in an Opticon Monitor (MJ Research/Bio-Rad). The numbering of the mutations in this work is based on *TGFBR2*, transcript variant 2 (NM_003242).

Structure modeling, mutation mapping and alignments

The kinase structure of TβRII was generated by homology modeling using SWISS-MODEL with ActRIIB (2QLU) as a template. Structures for ActRIIB (PDB: 2QLU), BMPR2 (PDB: 3G2F), Alk2 (PDB: 3H9R) and Alk5 (PDB: 1BC6, 1PY5) where displayed and superimposed using PyMol (Delano Scientific), and multiple sequence alignments were generated with BioEdit and ClustalW.

Cell culture and transfections

COS7 and HEK293T cells were maintained in DMEM with 10% FCS (PAA) at 10% CO_2 and DR26 mink lung cells in MEM with Earle's salts (PAA) supplemented with non-essential amino acids (Invitrogen) at 5% CO2. COS7 and HEK293T cells were transfected with polyethylenimine (Sigma-Aldrich); DR26 were transfected with JetPEI (Polyplus transfection) or Lipofectamine 2000 (Invitrogen) according to the manufacturers' instructions.

Cell lysis, western blotting and phosphoprotein assays

Twenty to 40 hours post-transfection, cells were lysed in 1× Laemmli SDS sample buffer, and lysates were stored at –20°C. After denaturing SDS-PAGE, proteins were blotted to PVDF membranes, membranes were blocked in 5% BSA and incubated overnight with the appropriate antibodies: anti-FLAG M2 (Sigma-Aldrich), anti-TβRII (Santa Cruz), anti-GAPDH, anti-histone H3, anti-pERK1/2 (Cell Signaling), anti-phospho-Smad2 (Zymed) at a 1:1000 dilution, followed by HRP-conjugated secondary antibodies goat-anti-mouse or goat-anti-rabbit (1:10000; Dianova), respectively. Chemoluminescent reactions were developed using Femto-Glo ECL reagents (PJK, Kleinblittersdorf, Germany) and documented on a ChemiSmart 5000 digital imaging system (Vilber-Lourmat). For phosphoprotein assays, HEK293T and DR26 cells were transfected as described above. Twenty hours after transfection, cells were starved for 4–6 hours in serum-free medium. Following stimulation with 200 pM TGF-β1 (Peprotech) for 5–40 minutes, cells were lysed in 1× Laemmli SDS sample buffer and analyzed by western blotting. Smad2, phospho-Smad2 and phospho-ERK1/2 proteins were quantified by volumetric measurements using the Bio1D software (Vilber-Lourmat/Peqlab) on raw images from a ChemiSmart 5000 digital imaging system (Vilber-Lourmat/Peqlab).

Nuclear and cytoplasmic fractionation and immunocytochemistry

HEK293T cells were harvested in ice-cold PBS. Fractionation was performed using the ProteoJet Extraction Kit (Fermentas) buffers with modifications to the manufacturer's protocol: briefly, the pellet was resuspended in 100 µl cytoplasmic lysis buffer, vortexed for 10 seconds and incubated on ice for 10 minutes. After vortexing for 10 seconds, nuclei were pelleted by centrifugation (7 minutes, 1000 ***g***). The supernatant cytosolic fraction was clarified by centrifugation (15 minutes, 20,000 ***g***). Nuclei were washed twice and lysed in nuclei storage buffer containing lysis reagent. After 15 minutes rotating at 4°C, the nuclear fraction was clarified as described. Immunocytochemistry was used to visualize Smad nuclear translocation. DR26 cells were co-transfected as described above in eight-well chamber slides (Nunc) with receptor expression constructs and a green fluorescent protein vector pEGFP-N1. Twenty hours post-transfection, cells were starved for 4 hours in serum-free medium and stimulated with 250 pM TGF-β1 for 30 minutes. Cells were fixed in 4% paraformaldehyde and stained with anti-Smad2 (1:200; Cell Signaling), followed by goat-anti-rabbit IgG Alexa Fluor 594 conjugate (1:300; Molecular Probes).

Cell surface staining and measurement of internalization

Twenty hours post-transfection, cells were harvested using 5 mM EDTA in PBS. HA-tagged TβRII was stained with anti-HA7 (Sigma-Aldrich) at 1 µg/10^6 cells in HEPES-buffered DMEM with 1% BSA for 40 minutes at 4°C. For measurement of cell surface expression, bound anti-HA7 was recognized by goat-anti-mouse IgG Alexa Fluor488 conjugate (Molecular Probes). Cells were resuspended in PBS containing propidium iodide (1 µg/ml; Sigma-Aldrich) for dead cell discrimination before measurement in an Epics XL-MCL flow cytometer (Beckman-Coulter). To monitor receptor internalization, surface TβRII was labelled with anti-HA7 as described. After washing with HEPES-buffered DMEM, cells were then either kept at 4°C or transferred to 37°C for various lengths of time. Dynasore (160 µM; Sigma-Aldrich) was used to prevent receptor internalization in control cells. Antibody-labeled TβRII remaining at the cells surface was visualized with goat-anti-mouse IgG Alexa Fluor 488. Cells were resuspended in PBS containing propidium-iodide and measured as described. Flow cytometry data were evaluated using FCSExpress (Denovo Software). Permeable, dead cells (PI positive) were excluded from analysis as well as cell aggregates (high forward-scatter) and nonviable or apoptotic cells that became apparent as an additional population with very low forward and high side-scatter. Fluorescence histograms are shown in the supplementary material Fig. S5.

In vitro kinase assay

FLAG-tagged TβRII was immunoprecipitated with anti-FLAG M2 (Sigma-Aldrich) from lysates of transiently transfected HEK293T cells in TNE lysis buffer containing PMSF, complete protease inhibitor cocktail (Roche) and NaF. TβRII was immunoprecipitated using anti-FLAG antibodies, followed by incubation with protein-A–sepharose. After centrifugation, sepharose pellets were resuspended in kinase buffer containing 5 µCi [γ-^{32}P]ATP (Hartmann Analytics) and incubated for 30 minutes at 30°C. Following SDS-PAGE and western blotting, signals were collected on film. The total quantity of receptors on the membrane was determined after decay of the radioactive ^{32}P signal using anti-FLAG and anti-TβRII antibodies, as described above.

Dual luciferase assays

DR26 cells were co-transfected with TβRII constructs, TGF-β-inducible p3TP-luc or p$(CAGA)_{12}$-luc reporters and a constitutively active renilla luciferase (pRLTK-luc) reporter construct in 96-well and 24-well plates, respectively, using JetPEI (Polyplus transfections). Twenty hours after transfection, cells were starved for 4 hours in EMEM containing 0.1% FCS before stimulation with 100 pM TGF-β1 (Peprotech) for 15 hours. Cells were lysed in passive lysis buffer (Promega), and luciferase activities were measured using the dual luciferase assay system (Promega) according to the manufacturer's instructions in a Mithras LB940 multimode plate reader (Berthold Technologies).

This work was supported by grants from the Deutsche Forschungsgemeinschaft (DFG SFB 760) to P.K. and P.N.R. and the European Commission (FAD; HEALTH-F2-2008-200647) to P.N.R. D.H. is supported by a Sonnenfeld fellowship. We thank Sonja Niedrig for excellent technical assistance and project students Maria Weinert and Robert Kudernatsch for their valuable support. We are grateful to Alex Bullock for discussions on the TβRII structure. We thank Yoav Henis for providing us with the TβRII AAA mutant.

Supplementary material available online at
http://jcs.biologists.org/cgi/content/full/123/24/4340/DC1

References

Arnold, K., Bordoli, L., Kopp, J. and Schwede, T. (2006). The SWISS-MODEL workspace: a web-based environment for protein structure homology modelling. *Bioinformatics* **22**, 195-201.

Attias, D., Stheneur, C., Roy, C., Collod-Béroud, G., Detaint, D., Faivre, L., Delrue, M.-A., Cohen, L., Francannet, C., Béroud, C. et al. (2009). Comparison of clinical presentations and outcomes between patients with TGFBR2 and FBN1 mutations in Marfan syndrome and related disorders. *Circulation* **120**, 2541-2549.

Bakin, A. V., Tomlinson, A. K., Bhowmick, N. A., Moses, H. L. and Arteaga, C. L. (2000). Phosphatidylinositol 3-kinase function is required for transforming growth factor beta-mediated epithelial to mesenchymal transition and cell migration. *J. Biol. Chem.* **275**, 36803-36810.

Barak, L. S., Tiberi, M., Freedman, N. J., Kwatra, M. M., Lefkowitz, R. J. and Caron, M. G. (1994). A highly conserved tyrosine residue in G protein-coupled receptors is required for agonist-mediated beta 2-adrenergic receptor sequestration. *J. Biol. Chem.* **269**, 2790-2795.

Borders, C. L., Broadwater, J. A., Bekeny, P. A., Salmon, J. E., Lee, A. S., Eldridge, A. M. and Pett, V. B. (1994). A structural role for arginine in proteins: multiple hydrogen bonds to backbone carbonyl oxygens. *Protein Sci.* **3**, 541-548.

Carcamo, J., Zentella, A. and Massagué, J. (1995). Disruption of transforming growth factor beta signaling by a mutation that prevents transphosphorylation within the receptor complex. *Mol. Cell. Biol.* **15**, 1573-1581.

Carta, L., Smaldone, S., Zilberberg, L., Loch, D., Dietz, H. C., Rifkin, D. B. and Ramirez, F. (2009). p38 MAPK is an early determinant of promiscuous Smad2/3 signaling in the aortas of Fibrillin-1 (Fbn1)-null mice. *J. Biol. Chem.* **284**, 5630-5636.

Chaudhry, S. S., Cain, S. A., Morgan, A., Dallas, S. L., Shuttleworth, C. A. and Kielty, C. M. (2007). Fibrillin-1 regulates the bioavailability of TGFbeta1. *J. Cell Biol.* **176**, 355-367.

Dennler, S., Itoh, S., Vivien, D., ten Dijke, P., Huet, S. and Gauthier, J. M. (1998). Direct binding of Smad3 and Smad4 to critical TGF beta-inducible elements in the promoter of human plasminogen activator inhibitor-type 1 gene. *EMBO J.* **17**, 3091-3100.

Disabella, E., Grasso, M., Marziliano, N., Ansaldi, S., Lucchelli, C., Porcu, E., Tagliani, M., Pilotto, A., Diegoli, M., Lanzarini, L. et al. (2006). Two novel and one known mutation of the TGFBR2 gene in Marfan syndrome not associated with FBN1 gene defects. *Eur. J. Hum. Genet.* **14**, 34-38.

Ehrlich, M., Shmuely, A. and Henis, Y. I. (2001). A single internalization signal from the di-leucine family is critical for constitutive endocytosis of the type II TGF-(beta) receptor. *J. Cell Sci.* **114**, 1777-1786.

Gomez, D., Zen, A. A. H., Borges, L. F., Philippe, M., Gutierrez, P. S., Jondeau, G., Michel, J.-B. and Vranckx, R. (2009). Syndromic and non-syndromic aneurysms of the human ascending aorta share activation of the Smad2 pathway. *J. Pathol.* **218**, 131-142.

Gordon, K. J. and Blobe, G. C. (2008). Role of transforming growth factor-beta superfamily signaling pathways in human disease. *Biochim. Biophys. Acta* **1782**, 197-228.

Gregory, K. E., Ono, R. N., Charbonneau, N. L., Kuo, C.-L., Keene, D. R., Bächinger, H. P. and Sakai, L. Y. (2005). The prodomain of BMP-7 targets the BMP-7 complex to the extracellular matrix. *J. Biol. Chem.* **280**, 27970-27980.

Guex, N. and Peitsch, M. C. (1997). SWISS-MODEL and the Swiss-PdbViewer: an environment for comparative protein modeling. *Electrophoresis* **18**, 2714-2723.

Habashi, J. P., Judge, D. P., Holm, T. M., Cohn, R. D., Loeys, B. L., Cooper, T. K., Myers, L., Klein, E. C., Liu, G., Calvi, C. et al. (2006). Losartan, an AT1 antagonist, prevents aortic aneurysm in a mouse model of Marfan syndrome. *Science* **312**, 117-121.

Han, S., Loulakis, P., Griffor, M. and Xie, Z. (2007). Crystal structure of activin receptor type IIB kinase domain from human at 2.0 Angstrom resolution. *Protein Sci.* **16**, 2272-2277.

Hasham, S. N., Willing, M. C., Guo, D. C., Muilenburg, A., He, R., Tran, V. T., Scherer, S. E., Shete, S. S. and Milewicz, D. M. (2003). Mapping a locus for familial thoracic aortic aneurysms and dissections (TAAD2) to 3p24-25. *Circulation* **107**, 3184-3190.

Jones, J. A., Spinale, F. G. and Ikonomidis, J. S. (2008). Transforming growth factor-beta signaling in thoracic aortic aneurysm development: a paradox in pathogenesis. *J. Vasc. Res.* **46**, 119-137.

Kornev, A. P. and Taylor, S. S. (2010). Defining the conserved internal architecture of a protein kinase. *Biochim. Biophys. Acta* **1804**, 440-444.

Kornev, A. P., Taylor, S. S. and Eyck, L. F. T. (2008). A helix scaffold for the assembly of active protein kinases. *Proc. Natl. Acad. Sci. USA* **105**, 14377-14382.

Law, C., Bunyan, D., Castle, B., Day, L., Simpson, I., Westwood, G. and Keeton, B. (2006). Clinical features in a family with an R460H mutation in transforming growth factor beta receptor 2 gene. *J. Med. Genet.* **43**, 908-916.

Lawler, S., Feng, X.-H., Chen, R.-H., Maruoka, E. M., Turck, C. W., Griswold-Prenner, I. and Derynck, R. (1997). The type II transforming growth factor-beta receptor autophosphorylates not only on serine and threonine but also on tyrosine residues. *J. Biol. Chem.* **272**, 14850-14859.

Lee, M. K., Pardoux, C., Hall, M. C., Lee, P. S., Warburton, D., Qing, J., Smith, S. M. and Derynck, R. (2007). TGF-beta activates Erk MAP kinase signalling through direct phosphorylation of ShcA. *EMBO J.* **26**, 3957-3967.

LeMaire, S. A., Pannu, H., Tran-Fadulu, V., Carter, S. A., Coselli, J. S. and Milewicz, D. M. (2007). Severe aortic and arterial aneurysms associated with a TGFBR2 mutation. *Nat. Clin. Pract. Cardiovasc. Med.* **4**, 167-171.

Loeys, B. L., Chen, J., Neptune, E. R., Judge, D. P., Podowski, M., Holm, T., Meyers, J., Leitch, C. C., Katsanis, N., Sharifi, N. et al. (2005). A syndrome of altered cardiovascular, craniofacial, neurocognitive and skeletal development caused by mutations in TGFBR1 or TGFBR2. *Nat. Genet.* **37**, 275-281.

Loeys, B. L., Schwarze, U., Holm, T., Callewaert, B. L., Thomas, G. H., Pannu, H., De Backer, J. F., Oswald, G. L., Symoens, S., Manouvrier, S. et al. (2006). Aneurysm syndromes caused by mutations in the TGF-beta receptor. *N. Engl. J. Med.* **355**, 788-798.

Luo, K. and Lodish, H. F. (1997). Positive and negative regulation of type II TGF-beta receptor signal transduction by autophosphorylation on multiple serine residues. *EMBO J.* **16**, 1970-1981.

Macia, E., Ehrlich, M., Massol, R., Boucrot, E., Brunner, C. and Kirchhausen, T. (2006). Dynasore, a cell-permeable inhibitor of dynamin. *Dev. Cell* **10**, 839-850.

McKusick, V. A. (1969). On lumpers and splitters, or the nosology of genetic disease. *Perspect. Biol. Med.* **12**, 298-312.

Mizuguchi, T., Collod-Béroud, G., Akiyama, T., Abifadel, M., Harada, N., Morisaki, T., Allard, D., Varret, M., Claustres, M., Morisaki, H. et al. (2004). Heterozygous TGFBR2 mutations in Marfan syndrome. *Nat. Genet.* **36**, 855-860.

Mulder, K. M. (2000). Role of Ras and Mapks in TGFbeta signaling. *Cytokine Growth Factor Rev.* **11**, 23-35.

Neptune, E. R., Frischmeyer, P. A., Arking, D. E., Myers, L., Bunton, T. E., Gayraud, B., Ramirez, F., Sakai, L. Y. and Dietz, H. C. (2003). Dysregulation of TGF-beta activation contributes to pathogenesis in Marfan syndrome. *Nat. Genet.* **33**, 407-411.

Ng, J. (2008). TGFbeta signals regulate axonal development through distinct Smad-independent mechanisms. *Development* **135**, 4025-4035.

Pannu, H., Fadulu, V. T., Chang, J., Lafont, A., Hasham, S. N., Sparks, E., Giampietro, P. F., Zaleski, C., Estrera, A. L., Safi, H. J. et al. (2005). Mutations in transforming growth factor-beta receptor type II cause familial thoracic aortic aneurysms and dissections. *Circulation* **112**, 513-520.

Robinson, P. N., Arteaga-Solis, E., Baldock, C., Collod-Beroud, G., Booms, P., De Paepe, A., Dietz, H. C., Guo, G., Handford, P. A., Judge, D. P. et al. (2006). The molecular genetics of Marfan syndrome and related disorders. *J. Med. Genet.* **43**, 769-787.

Ross, S. and Hill, C. S. (2008). How the Smads regulate transcription. *Int. J. Biochem. Cell Biol.* **40**, 383-408.

Schwede, T., Kopp, J., Guex, N. and Peitsch, M. C. (2003). SWISS-MODEL: An automated protein homology-modeling server. *Nucleic Acids Res.* **31**, 3381-3385.

Singh, K. K., Rommel, K., Mishra, A., Karck, M., Haverich, A., Schmidtke, J. and Arslan-Kirchner, M. (2006). TGFBR1 and TGFBR2 mutations in patients with features of Marfan syndrome and Loeys-Dietz syndrome. *Hum. Mutat.* **27**, 770-777.

Sirard, C., Kim, S., Mirtsos, C., Tadich, P., Hoodless, P. A., Itié, A., Maxson, R., Wrana, J. L. and Mak, T. W. (2000). Targeted disruption in murine cells reveals variable requirement for Smad4 in transforming growth factor beta-related signaling. *J. Biol. Chem.* **275**, 2063-2070.

Sorrentino, A., Thakur, N., Grimsby, S., Marcusson, A., von Bulow, V., Schuster, N., Zhang, S., Heldin, C.-H. and Landström, M. (2008). The type I TGF-beta receptor engages TRAF6 to activate TAK1 in a receptor kinase-independent manner. *Nat. Cell Biol.* **10**, 1199-1207.

ten Dijke, P. and Arthur, H. M. (2007). Extracellular control of TGFbeta signalling in vascular development and disease. *Nat. Rev. Mol. Cell Biol.* **8**, 857-869.

Verrecchia, F. and Mauviel, A. (2002). Transforming growth factor-beta signaling through the Smad pathway: role in extracellular matrix gene expression and regulation. *J. Invest. Dermatol.* **118**, 211-215.

Wang, Q., Villeneuve, G. and Wang, Z. (2005). Control of epidermal growth factor receptor endocytosis by receptor dimerization, rather than receptor kinase activation. *EMBO Rep.* **6**, 942-948.

Wells, R. G., Yankelev, H., Lin, H. Y. and Lodish, H. F. (1997). Biosynthesis of the type I and type II TGF-beta receptors. Implications for complex formation. *J. Biol. Chem.* **272**, 11444-11451.

Wieser, R., Attisano, L., Wrana, J. L. and Massagué, J. (1993). Signaling activity of transforming growth factor beta type II receptors lacking specific domains in the cytoplasmic region. *Mol. Cell. Biol.* **13**, 7239-7247.

Wilkes, M. C., Mitchell, H., Penheiter, S. G., Doré, J. J., Suzuki, K., Edens, M., Sharma, D. K., Pagano, R. E. and Leof, E. B. (2005). Transforming growth factor-beta activation of phosphatidylinositol 3-kinase is independent of Smad2 and Smad3 and regulates fibroblast responses via p21-activated kinase-2. *Cancer Res.* **65**, 10431-10440.

Wrana, J. L., Attisano, L., Cárcamo, J., Zentella, A., Doody, J., Laiho, M., Wang, X. F. and Massagué, J. (1992). TGF beta signals through a heteromeric protein kinase receptor complex. *Cell* **71**, 1003-1014.

Wrana, J. L., Attisano, L., Wieser, R., Ventura, F. and Massagué, J. (1994). Mechanism of activation of the TGF-beta receptor. *Nature* **370**, 341-347.

Wu, M. Y. and Hill, C. S. (2009). TGF-beta superfamily signaling in embryonic development and homeostasis. *Dev. Cell* **16**, 329-343.

Yamashita, M., Fatyol, K., Jin, C., Wang, X., Liu, Z. and Zhang, Y. E. (2008). TRAF6 mediates smad-independent activation of JNK and p38 by TGF-beta. *Mol. Cell* **31**, 918-924.

Yin, S., Ding, F. and Dokholyan, N. V. (2007). Eris: an automated estimator of protein stability. *Nat. Methods* **4**, 466-467.

Zhang, Y. E. (2009). Non-Smad pathways in TGF-beta signaling. *Cell Res.* **19**, 128-139.